Evolution of the Polarizing Effect of MoS$_2$

S. Sathiyan
H. Ahmad
W. Y. Chong
S. H. Lee
S. Sivabalan
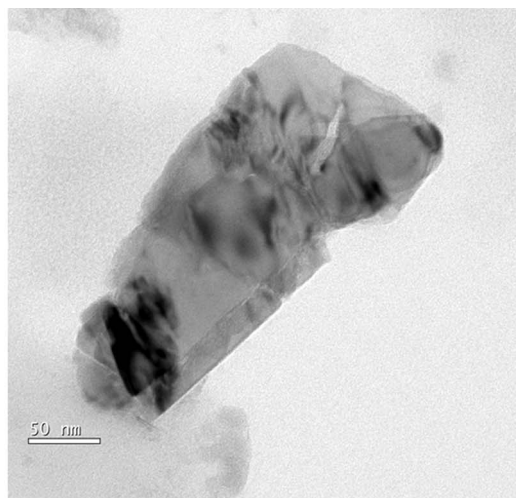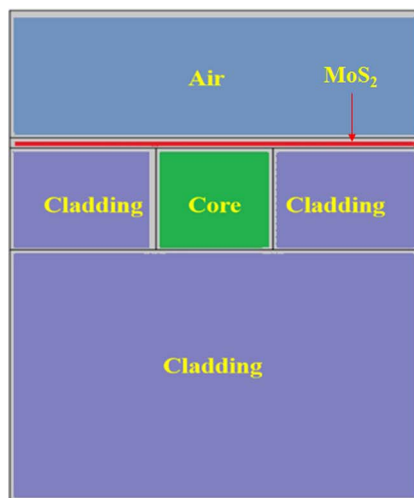
Evolution of the Polarizing Effect of MoS$_2$

S. Sathiyan,[1] H. Ahmad,[2] W. Y. Chong,[2] S. H. Lee,[2] and S. Sivabalan[1]

[1]School of Electrical Engineering, Vellore Institute of Technology University, Vellore-632 014, India
[2]Photonics Research Center, Department of Physics, Faculty of Science,
University of Malaya, 50603 Kuala Lumpur, Malaysia

Abstract: We have explored the polarization behavior of MoS$_2$ at three different wavelengths using a polymer-based waveguide. The MoS$_2$-coated waveguide has been fabricated based on the drop casting method. The maximum polarization extinction ratio of 12.6 dB that is achieved at 980 nm is considered to be the highest, to the best of our knowledge, for the MoS$_2$-based waveguide polarizer. It exhibits transverse electric (TE) pass characteristics in the visible wavelength region. The mode field confinement has been computed based on the finite-element method (FEM). Both numerical and experimental results are in very good agreement. These results demonstrate that the few-layer MoS$_2$ can be considered as a complementary material for graphene-based polarizers.

Index Terms: Molybdenum disulfide, polarization, planar optical waveguide.

1. Introduction

Polarization is an essential function in photonic integrated circuits (PICs), laser photonics, and optical communication systems. Polarization-based devices in PICs are the key components in optical signal processing, communication, and sensing applications [1]. The devices such as polarization controllers, polarization beam splitters, and polarizers are used as the polarization controlling devices in the optical integrated circuits for performing various optical functions [2]. In these, the polarizer is used to allow a single polarization i.e., either transverse electric (TE) or transverse magnetic (TM) into the circuit. This can be achieved by having higher loss for one mode compare to the other. The loss can be incurred by means of leakage or absorption and eventually results in high PER which is defined as the ratio of transmitted power of the desired polarization to the undesired polarization [3]. In the past, it has been reported that by using a metal dielectric waveguide, the plasmonic modes are generated and depends strongly on the polarization. This results in higher loss for one of the mode compare to the other. However, to achieve, broadband response using this technique require a complex structure with buffer layers [4]. In recent years, there has been much interest in graphene-based waveguide devices in PIC due to its remarkable electronic and optical properties. The unique properties of graphene such as broad optical bandwidth and very simple structure have attracted for devising waveguide based polarizer. Bao *et al.* have reported the first broadband polarizer with graphene as the thin layer coated onto an optical fiber, resulted in higher PER of 27 dB at 1550 nm wavelength with ~3 mm length of graphene [5]. Furthermore, the fabrication process of fiber based polarizer is

quite complicated, and it is difficult to integrate the fiber polarizer into the PIC. As the next step, Kim and Choi have experimentally demonstrated a graphene based polymeric integrated wave-guide polarizer operating at 1.31 μm with a graphene coating length of ~7 mm, in which the po-larizing characteristics changes from TE-pass (~10 dB PER) to TM-pass (~19 dB PER) when an upper cladding made of dielectric is added [6]. Later, Kou *et al.* reported the TM-pass behavior in an integrated silicon waveguide with graphene as the coating material resulted with a PER of 40 dB/mm around 1550 nm [7]. Lim *et al.* demonstrated a polymer optical waveguide polarizer coated with graphene oxide (GO) and achieved the maximum PER of 40 dB at 1590 nm wave-length. The length and thickness of the GO film is 1.3 mm and 2.0 μm, respectively [8]. Recently, Pei *et al.* demonstrated a broadband graphene/glass hybrid waveguide polarizer based on planar-light wave-circuit (PLC) with a maximum PER of ~27 dB at 1550 nm wavelength [9]. These im-pressive results shows that the graphene based waveguide is one of the promising PIC devices.

Very recently, there is a significant research interest in the transition metal dichalcogenides (TMDs) 2-D nanomaterial which is the derivatives of graphene. Compared to the graphene, TMDs have strong direct and in-direct bandgaps which are extensively used in electronic and optoelectronics device realization. Specifically, molybdenum disulfide (MoS_2) is one of the TMDs semiconducting materials which has gained much attention in recent years due its remarkable optical and electronic properties. Furthermore, MoS_2 has been widely used to develop future de-vices such as saturable absorber [10], [11], energy storage device [12], ultra-high gain photo detectors [13], transistors [14], and polarization dependent optical sensors [15]. In particular, the work on optical sensors showed potential polarization effects in MoS_2 when light propagates paral-lel to the film's plane. Further, the ion-implanted Nd: YAG crystal waveguide resulted in a maxi-mum PER of 4.9 dB/cm in the visible wavelength region for the MoS_2 length of ~10 mm. However, there is no report on the performance of waveguide polarizers using MoS_2-coated D-shaped optical fiber or planar waveguides, etc. since these types of polarizers are compact and easy to handle and implement.

In this work, the preliminary study of MoS_2 based waveguide polarizer has been done to ex-plore its polarizing properties at different wavelengths. SU-8 polymer strip waveguide is used for the analysis. The MoS_2 is coated using drop casting method which has been considered as the familiar method for graphene and graphene oxide coating [8]. The existence of polarization property has been studied with three different wavelengths namely 650 nm, 793 nm, and 980 nm. The maximum polarization extinction ratio of 12.6 dB is achieved at the wavelength of 980 nm is considered to be the highest to the best of our knowledge for MoS_2-based waveguide polarizer. Also, we have computed the mode field confinement in the waveguide using the finite element method (FEM) based tool. The numerical results are in good agreement with the experimental values. From the numerical and experimental analysis we have confirmed that the polymer wave-guide coated with MoS_2 exhibits TE-pass characteristics.

2. Material Preparation and Characterization

The few-layer MoS_2 have unique properties compared to bulk, as their bandgaps are different. Therefore, it is important to exfoliate the few-layer from the bulk material. Several approaches including micro mechanical cleavage, CVD, and solution-based methods are available to exfoli-ate the bulk materials. Among these methods, liquid phase exfoliation (LPE) is considered to be as most efficient and cost effective approach since it does not require any post-chemical treat-ments of the prepared solvents, and eventually, large-scale production is possible [16]. There-fore, we have adopted the LPE method to exfoliate the few-layer MoS_2 from bulk.

In brief, the bulk MoS_2 is mixed with N-methyl-pyrrolidone (NMP) solvent with an initial concen-tration of 5 mg/ml [17]. The solution is sonicated for 8 hours to break the weak van der Waals forces between the layers using a bath ultrasonicator. The suspension is then centrifuged at 3000 rpm for 60 minutes and the supernatant is extracted from the suspension to get the few-layer MoS_2.

The obtained supernatant solution is diluted to 10 vol % and the linear optical absorption characterization is carried out using Hitatchi-U-2800 UV/Vis Spectrophotometer.
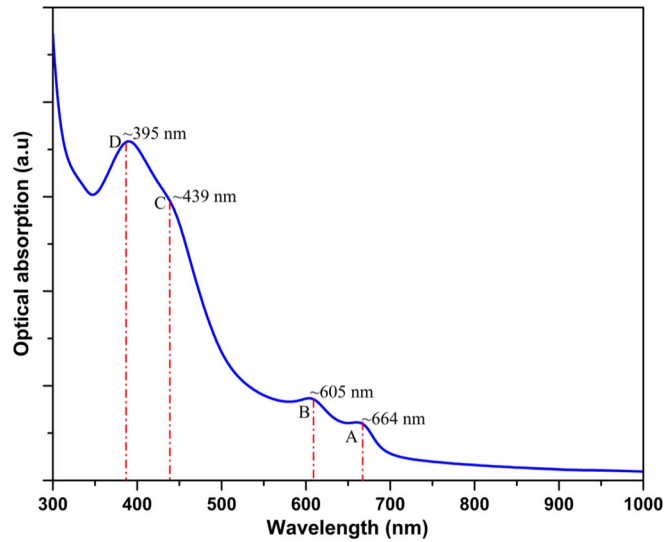
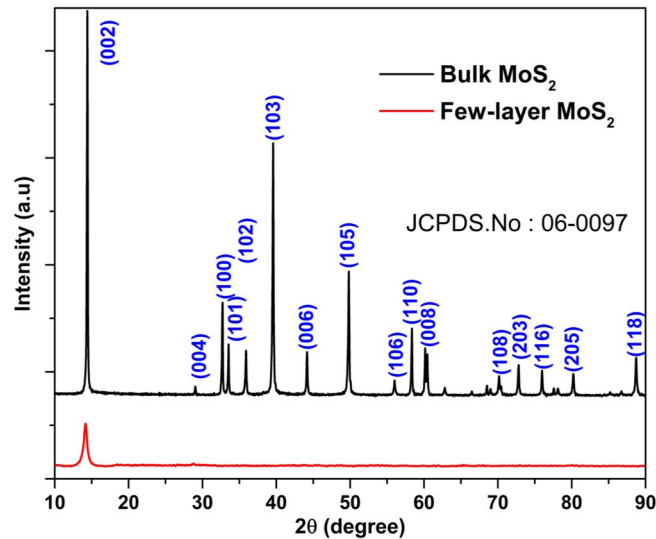Fig. 1. Linear optical absorption characterization of few-layer MoS$_2$ suspension diluted to 10 vol %.

Fig. 2. XRD analysis of bulk and few-layer MoS$_2$.

As seen in Fig. 1, the four observed peaks at ~664 nm (A), ~605 nm (B), ~439 nm (C), and ~395 nm (D) matched very well with the previous report [18]. In these, A and B transitions originate from the inter-band excitonic transitions which indicates 2H poly-type structure. On the other hand, C and D results from the transitions between higher density of states of the MoS$_2$ band structure. From this analysis, it is confirmed that the few-layer MoS$_2$ nanosheets are exfoliated from the bulk.

Next, we proceed to confirm the crystalline nature of few-layer MoS$_2$ nanosheets with the XRD analysis using Bruker D8 Advanced machine at an excitation wavelength of 1.5406 Å. The few-layer MoS$_2$ solution is drop casted onto a quartz substrate and annealed at 400 °C for 10 minutes. The prepared sample is characterized with XRD and the result is presented in Fig. 2. From the figure, it is very clear that all the labeled major peaks of bulk MoS$_2$ (black) perfectly indexed to rhombohedral MoS$_2$ (JCPDS No: 06-0097). Further, the few-layer MoS$_2$ (red) shows a
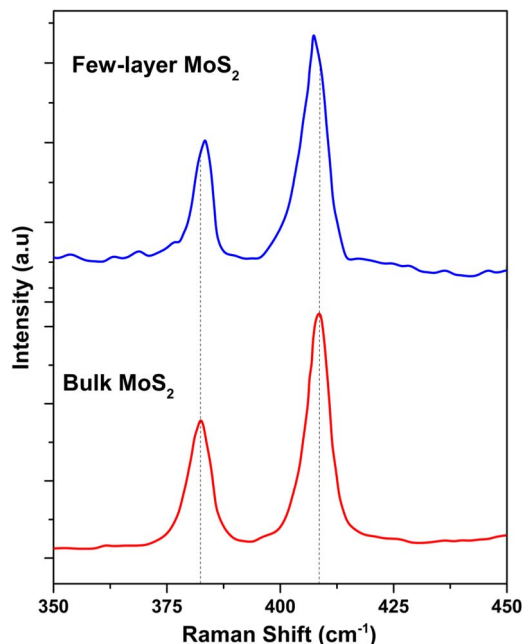
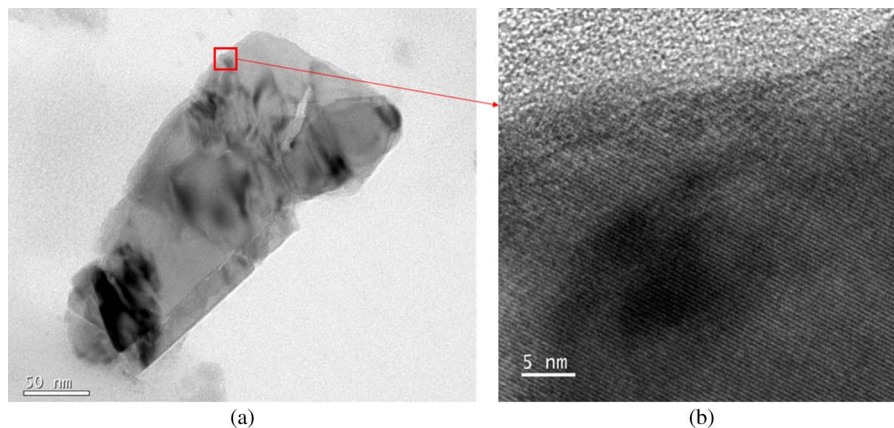Fig. 3. Raman spectroscopy characterization of bulk and few-layer MoS$_2$.

Fig. 4. Transmission electron microscope (TEM) images of the MoS$_2$ flakes with (a) 50 nm and (b) 5 nm resolutions.

very high [002] orientation with the disappearance of some peaks. These results confirms the existence of few-layer MoS$_2$ nanosheets.

As the next step we characterized the Raman spectroscopy using Renishaw inVia Raman microscope at an excitation wavelength of 488 nm with a power of 1.5 mW. The samples are prepared by drop casting the solution onto the silica wafers. In Fig. 3, the two main Raman peaks at 383 cm^{-1} and 407 cm^{-1} correspond to the in-plane (E_{2g}^{1}) and out-of plane (A_{1g}) vibrational modes of the few-layer MoS$_2$. It can be observed that there is a shift of peak for few-layer MoS$_2$ compared to the bulk and it is calculated as 24 cm^{-1} which corresponds to the number of layers of about ~4-5 (as the single layer thickness of MoS$_2$ is 0.65 nm [19]).

The morphological characterization of the exfoliated MoS$_2$ nanosheets are analyzed using transmission electron microscope (TEM, FEI Tecnai G2 F20) with a scale of 50 nm and 5 nm, as shown in Fig. 4(a) and (b), respectively. From the figures, it is very clear that the 2-D nanosheets
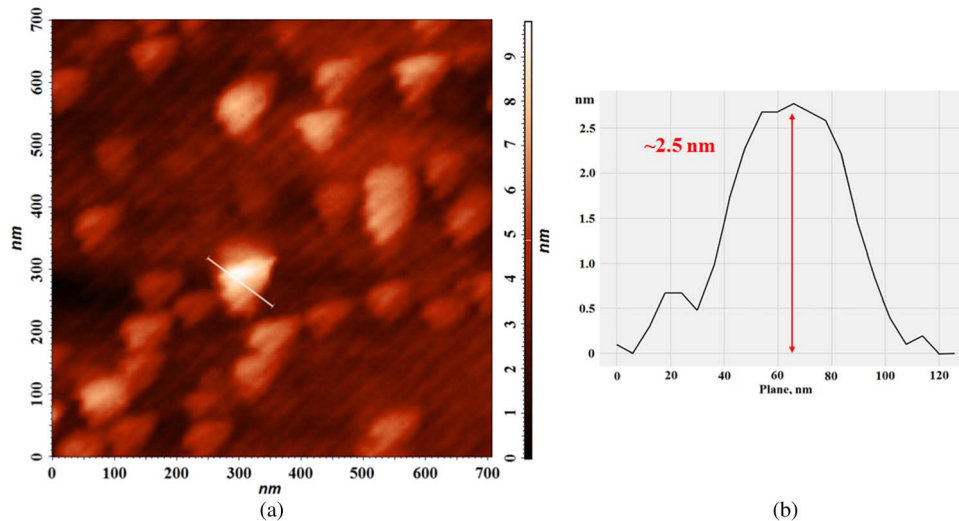
Fig. 5. (a) AFM measurements of the MoS$_2$ nanosheets. (b) Corresponding height profile diagram.

with the size of a few hundreds of nanometers with good uniformity have been obtained. These results further confirm the typical layered structure with the presence of the high quality few-layer MoS$_2$ nanosheets exfoliated through LPE method.

Further, the thickness of the exfoliated MoS$_2$ nanosheets is characterized using Atomic Force Microscopy (AFM, NT-MDT) as shown in Fig. 5. From the height profile diagram [see Fig. 5(b)], the average thickness is measured as ~2.5 nm, which confirms the number of layers to be around ~4 to 5 layers. These results strongly validates the exfoliation of few-layer MoS$_2$ from the bulk and matches with the Raman spectroscopy data.

3. Waveguide Preparation and Coating

The strip waveguide is formed by using SU8-2010 polymer which acts as the core and cladding materials. The bottom cladding is spin-coated onto a silicon wafer substrate at 2000 rpm and baked at 83 °C for 2 min using a hotplate. It is then flood exposed using multi-line mercury lamp followed by a second baking at 83 °C for 40 sec. The core layer is then spin-coated onto the bottom cladding layer using SU-8 2010 which is diluted with cyclopentanone (7 : 3) by volume to produce a coating thickness of around 8 μm. It is then soft baked at 83 °C for 30 min followed by 10 min cool down to ambient temperature. Subsequently, the sample undergoes UV exposure using hard contact mask lithography patterning. The sample is baked for a second time, starting at 56 °C for 20 s followed by 30 °C/min ramp to a final temperature of 140 °C. The sample is then UV flood exposed again and post-exposure baked (PEB) starting at 56 °C for 20 sec, followed by 30 °C/min ramp to 83 °C to create the strip waveguide.

3.1. Coating of MoS$_2$

Next, the coating of MoS$_2$ is carried out using the drop casting method. The estimated concentration of the solution is around ~0.07 mg/ml. We have drop casted the MoS$_2$ solution using a precision micropipette. Briefly, 1 μl of the MoS$_2$ solution is drop casted on the waveguide channel followed by heat treatment for 15 min at 90 °C. The five waveguide channels are drop casted with different number of drops on each channel. It is observed that when the MoS$_2$ solution is drop casted on the waveguide, it tends to spread over the surface of the waveguide channel due to the weak surface tension of the NMP solvent. However, we have drop casted the solution at the same position after each proceeding drops have dried off. Also, the spreading can be avoided by using difference solvents whose surface tension is comparable to the waveguide material. The thickness of each coating is then measured using DEKTAK D150 step profiler. The
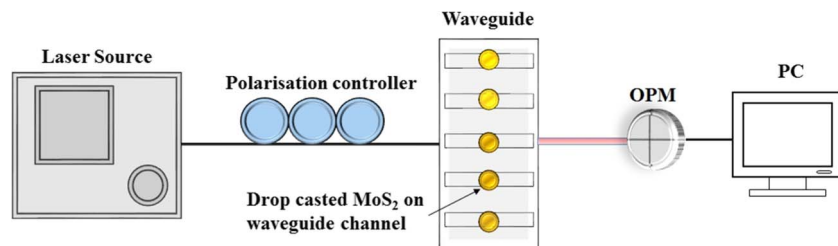
Fig. 6. Experimental setup to measure the insertion loss and polarization dependent loss.
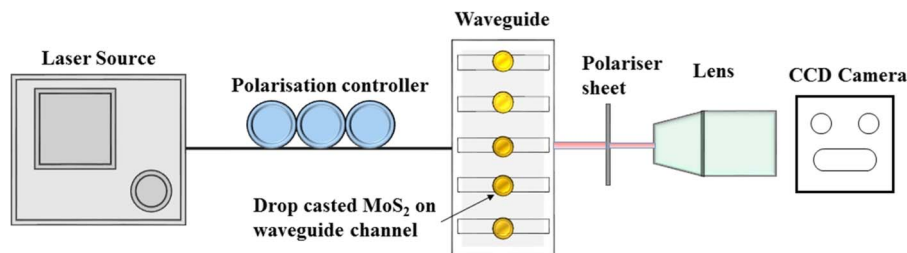

Fig. 7. Experimental setup to measure the polarization state.

average thickness of the MoS$_2$ coating lies in the range between 0.5 μm to 1.65 μm. Here, we are intent to record that the thickness of the coating is the average of the repeated measurements. This is because of the surface profiler tip which has a tendency of scratching the coating surface and eventually complicates the absolute thickness measurement.

4. Experimental Setup and Discussion

Fig. 6. shows the schematic experimental setup to measure the polarization performance of the MoS$_2$ coated waveguide polarizer. Three different laser diodes emitting at wavelength of 650 nm, 793 nm and 980 nm were used in the measurement. The inline polarization controller is used to tune the polarization of the laser source. The insertion loss and polarization dependent loss for the bare waveguide is measured using butt-coupling method and it is found to be −13.2 dB and 0.5 dB respectively.

An experimental setup as shown in Fig. 7 is used to confirm the polarization state at the output of the waveguide. As it is obvious from the figure, a free space polarizer is placed after the waveguide and the objective lens is used to focus the light into the CCD camera. The waveguide exhibits TE polarization, and these results are further confirmed by the numerical analysis, which is discussed later in this section.

For each channel, the insertion loss and polarization dependent loss has been measured after the MoS$_2$ coating and the results are portrayed in Figs. 8 and 9. For 980 nm, the insertion loss increases linearly with the addition of number of drops. The similar variation is occurring for 793 nm and 650 nm with a sudden dip in the second coating. We believe that the variation may be caused by uneven coating on the second waveguide channel. Due to the non-inversion symmetry structure of MoS$_2$, it exhibits strong spin coupling and valley confinement. Because of that, the imaginary part of the dynamic conductivity lies in the visible range [15]. We have tried to measure the polarization dependent loss for 1.31 μm and 1.55 μm wavelengths, but the change in the polarization dependent loss is not significant for these wavelengths. This is because the bandgap of MoS$_2$ lies in the range between 1.29 eV (961 nm) to 1.80 eV (689 nm). Therefore, the absorption of light for MoS$_2$-based waveguide polarizer lies in the above specified wavelength range. These results are in good agreement with the previously reported values [15].

Next, we measured the extinction ratio, the difference between the maximum power and the minimum power observed by adjusting the polarization controller. We achieved a maximum
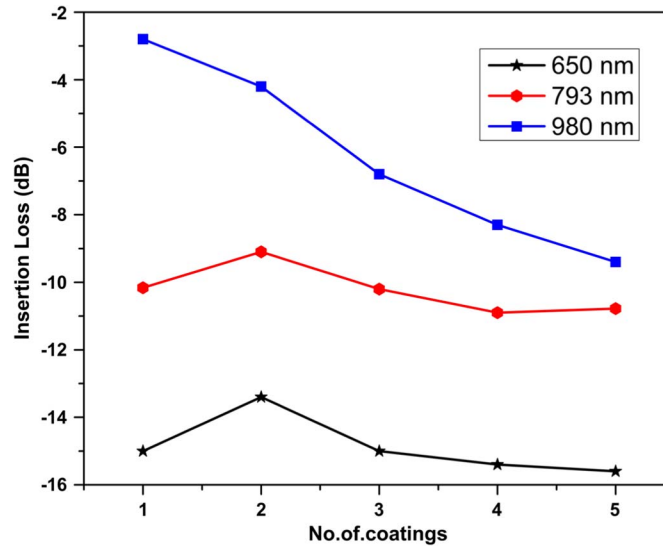
Fig. 8. Variation of insertion loss with respect to number of drop coating for 650 nm, 793 nm, and 980 nm.
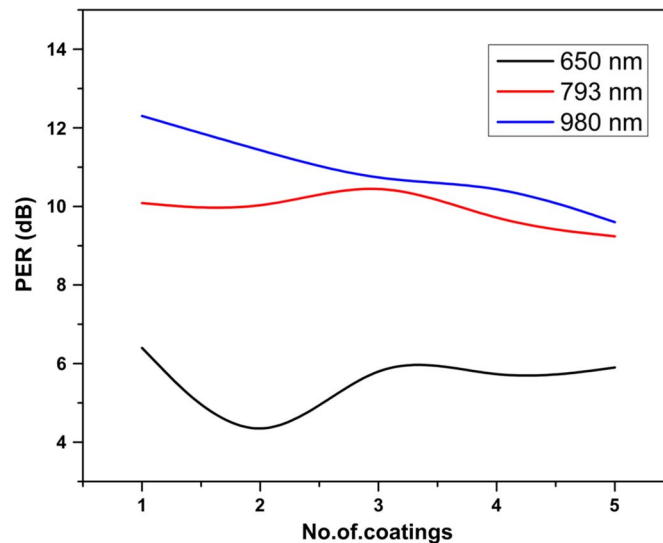

Fig. 9. Variation of polarization dependent loss against number of drops coated for 650 nm, 793 nm, and 980 nm wavelengths.

extinction ratio of 12.6 dB at 980 nm for one drop coating. The variation of extinction ratio as the function of number of coatings is depicted in Fig. 9. Repeated measurements were taken over a period of one week and it was found that the results are consistent for all measurements.

5. Numerical Modeling and Analysis

We have computed the mode field confinement of the MoS$_2$ coated waveguide polarizer using a finite element method software COMSOL Multiphysics v5.0. The schematic cross section of the waveguide coated with MoS$_2$ is shown in the Fig. 10. The typical waveguide dimensions are 8 μm height and 8 μm width. The thickness of the MoS$_2$ is varied according to the drops of the MoS$_2$ added. We assumed that the thickness of MoS$_2$ is uniform along the waveguide section.
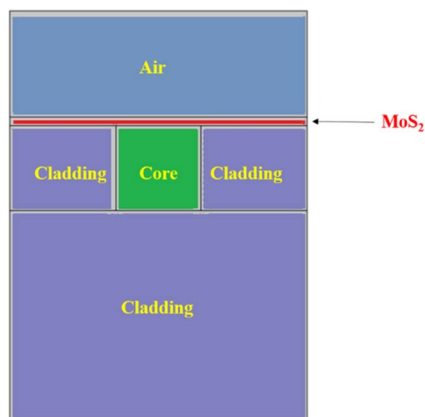
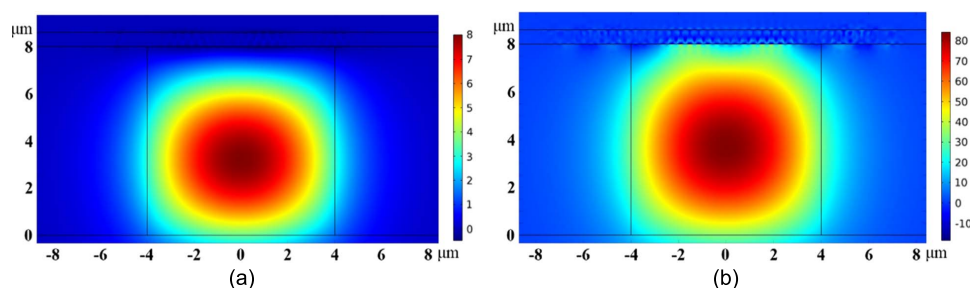Fig. 10. Schematic representation of waveguide structure.

Fig. 11. (a) Mode field distribution of electric field x-component and (b) mode field distribution of electric field y-component.

Zhang *et al.*, has devised a method to extract the complex refractive index of MoS$_2$ in the visible wavelength region by means of contrast spectra [20]. At 650 nm, the measured value of complex refractive index is $4.49 - 1.01i$, and the same is used in the simulation. The simulation computes the complex propagation constant, $\{\mathrm{Re}\,(n_{\mathrm{eff}}) + i\,\mathrm{Im}(n_{\mathrm{eff}})\}$ corresponding to the fundamental mode field distribution for electric field x-component and electric field y-component. The attenuation value is calculated by the imaginary part of n_{eff} i.e., $\alpha = \mathrm{Im}\,(n_{\mathrm{eff}})^*\mathrm{k}0$, where α is the attenuation coefficient, and k0 is the wave number. The thickness of the MoS$_2$ is varied between $0.5 - 1.65\ \mu$m. Effects of surface roughness on the performance were not considered in the simulation. Fig. 11(a) and (b) shows the fundamental mode distribution for electric field x-component and electric field y-component, respectively. The electric field y-component has higher loss when compared to the electric field x-component.

From this analysis, we can conclude that the waveguide polarizer exhibits transverse electric polarization (TE). The polarization extinction ratio between the TE and TM polarization for 650 nm is computed and plotted in Fig. 12. From the figure, it is apparent that both experimental and theoretical curves show a similar trend except at two drop coating. As discussed earlier, this change may arise because of the uneven coating on the particular waveguide. The lower measured PER compared to simulation results is attributed to the surface roughness of the MoS$_2$ coating.

6. Conclusion

In this report, we have analyzed the polarizing characteristics of MoS$_2$ coated on a polymer waveguide through drop casting method in the visible wavelength range. The waveguide polarizer exhibits TE-pass characteristics with a maximum PER of 12.6 dB at 980 nm, which is the highest for the MoS$_2$-based waveguide polarizer, to the best of our knowledge. In addition, we have
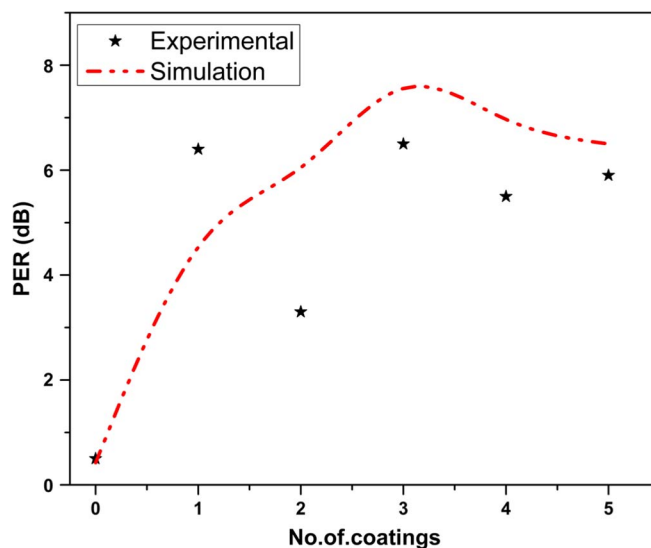
Fig. 12. Experimental and theoretical comparison of polarization dependent loss (extinction ratio) with respect to number of coatings at 650 nm.

carried out a numerical simulation based on the finite element method. The experimental results are in very good agreement with the theoretical results. The few-layer MoS$_2$ can be considered as a complementary material for graphene based polarization studies.

References

[1] S. M. Ojha *et al.*, "Simple method of fabricating polarisation-insensitive and very low crosstalk AWG grating devices," *Electron. Lett.*, vol. 34, no. 1, pp. 78–79, Jan. 1988.

[2] D. C. Hutchings and B. M. Holmes, "A waveguide polarization toolset design based on mode beating," *IEEE Photon. Technol. Lett.*, vol. 3, no. 3, pp. 450–461, Jun. 2011.

[3] J.-J. He *et al.*, "Integrated polarization compensator for WDM waveguide demultiplexers," *IEEE Photon. Technol. Lett.*, vol. 11, no. 2, pp. 224–226, Feb. 1999.

[4] D. Dai, Z. Wang, N. Julian, and J. E. Bowers, "Compact broadband polarizer based on shallowly-etched silicon-on-insulator ridge optical waveguides," *Opt. Exp.*, vol. 18, no. 26, pp. 27404–27415, Dec. 2010.

[5] Q. Bao *et al.*, "Broadband graphene polarizer," *Nat. Photon.*, vol. 5, no. 7, pp. 411–415, Jul. 2011.

[6] J. T. Kim and C. G. Choi, "Graphene-based polymer waveguide polarizer," *Opt. Exp.*, vol. 20, no. 4, pp. 3556–3562, Feb. 2012.

[7] R. Kou *et al.*, "Characterization of optical absorption and polarization dependence of single-layer graphene integrated on a silicon wire waveguide," *Jpn. J. Appl. Phys.*, vol. 52, no. 6R, May 2013, Art. ID 060203.

[8] W. H. Lim *et al.*, "Graphene oxide-based waveguide polariser: From thin film to quasi-bulk," *Opt. Exp.*, vol. 22, no. 9, pp. 11090–11098, May 2014.

[9] C. Pei *et al.*, "Broadband graphene/glass hybrid waveguide polarizer," *IEEE Photon. Technol. Lett.*, vol. 27, no. 9, pp. 927–930, May 2015.

[10] H. Zhang *et al.*, "Molybdenum disulfide (MoS$_2$) as a broadband saturable absorber for ultra-fast photonics," *Opt. Exp.*, vol. 22, no. 6, pp. 7249–7260, Mar. 2014.

[11] H. Liu *et al.*, "Femtosecond pulse erbium-doped fiber laser by a few-layer MoS$_2$ saturable absorber," *Opt. Lett.*, vol. 39, no. 15, pp. 4591–4594, Aug. 2014.

[12] G. S. Bang *et al.*, "Effective liquid-phase exfoliation and sodium ion battery application of MoS$_2$ nanosheets," *ACS Appl. Mater. Interfaces*, vol. 6, no. 10, pp. 7084–7089, Apr. 2014.

[13] O. L- Sanchez, D. Lembke, M. Kayci, A. Radenovic, and A. Kis, "Ultrasensitive photodetectors based on monolayer MoS$_2$," *Nat. Nanotechnol.*, vol. 8, no. 7, pp. 497–501, Jul. 2013.

[14] D. Krasnozhon, D. Lembke, C. Nyffeler, Y. Leblebici, and A. Kis, "MoS$_2$ transistors operating at gigahertz frequencies," *Nano Lett.*, vol. 14, no. 10, pp. 5905–5911, Sep. 2014.

[15] Y. Tan *et al.*, "Polarization-dependent optical absorption of MoS$_2$ for refractive index sensing," *Sci. Rep.*, vol. 4, p. 7523, 2014.

[16] V. Nicolosi, M. Chhowalla, M. G. Kanatzidis, M. S. Strano, and J. N. Coleman, "Liquid exfoliation of layered materials," *Science*, vol. 340, no. 6139, Jun. 2013, Art. ID 1226419.

[17] N. Dong *et al.*, "Optical limiting and theoretical modelling of layered transition metal dichalcogenide nanosheets," *Sci. Rep.*, vol. 5, p. 14646, 2015.

[18] R. I. Woodward *et al.*, "Tunable Q-switched fiber laser based on saturable edge-state absorption in few-layer molybdenum disulfide (MoS$_2$)," *Opt. Exp.*, vol. 22, no. 25, pp. 31113–31122, Dec. 2014.

[19] B. Radisavljevic, A. Radenovic, J. Brivio, V. Giacometti, and A. Kis, "Single-layer MoS$_2$ transistors," *Nat. Nanotechnol.*, vol. 6, no. 3, pp. 147–150, Feb. 2011.

[20] H. Zhang *et al.*, "Measuring the refractive index of highly crystalline monolayer MoS$_2$ with high Confidence," *Sci. Rep.*, vol. 5, p. 8440, Feb. 2015.